



Development of High-resolution EEG Devices

Thomas C. Ferree^{a,b} and Don M. Tucker^{a,b}

^a*Electrical Geodesics, Inc., Riverfront Research Park, Eugene, OR 97403*

^b*Department of Psychology, University of Oregon, Eugene, OR 97403*

Abstract. In this paper, we describe a new direction in the advancement of dense-array EEG technology. It is generally accepted that three-dimensional spatial analysis of EEG via electric head models requires accurate representation of both head geometry and head tissue conductivity. Anatomical information can be obtained from structural MRI. At present, however, most researchers still take conductivity parameters from standard references, despite the large variability in the available data. We have therefore developed a method for estimating regional head tissue conductivities in vivo, by injecting small (1–10 mA) currents into the head, and measuring the electric potential at the remaining electrodes of a dense-array EEG net. Despite the obvious fact that most current is shunted through the scalp, our results demonstrate that regional head tissue conductivities can be estimated to within a few percent error.

1. Introduction

The development of high-resolution electroencephalography (EEG) involves advancements in both device technology and analysis methods and software. Regarding devices, the efforts of our group are focused mainly on the development of the Geodesic Sensor Net and the Net Amps amplifier system. The Geodesic Sensor Net (GSN) is a dense sensor array of 128 or 256 electrodes with approximately equal spacing between adjacent pairs [16]. Figure 1 shows that, in addition to providing high spatial resolution, the design of this net solves a number of practical problems. It is quick and easy to apply, does not require skin abrasion, and can be worn comfortably for hours. In addition to ease of use in research settings, recent studies at the Sacred Heart Medical Center in Eugene, Oregon, show that the GSN is also practical and reliable for clinical use [8].



Figure 1. Application of the 128-channel Geodesic Sensor Net.

The voltage signals are amplified by the Net Amps, which are designed specifically for use with the GSN. While high-resolution EEG promises to enable researchers and clinicians to study patterns of brain activity not detectable with conventional electrode arrays [14], several technological challenges remain to make maximal use of this rich data.

Primary among these challenges is the fact that accurate three-dimensional spatial analysis of EEG data via electric head models requires accurate representation of both head geometry and regional head tissue conductivity [1,11,12,15]. Although early head models assumed spherical head geometry, modern boundary element [10] and finite element methods allow the incorporation of realistic head geometry. Modulo the technical challenges of automated tissue segmentation, structural MRI can provide the necessary anatomical information for accurate head models. In both spherical and realistic models, the head is usually represented electrically as four homogeneous and isotropic conductive regions. Table 1 shows the ranges of these regional tissue conductivities, tabulated from the experimental literature [2,5,7].

Table 1. Head tissue conductivity (1/Wm) tabulated from the experimental literature.

Tissue	Mean s	Stdev s	Min s	Max s
Brain	0.25	0.13	0.05	1.0
CSF	1.79	0.02	1.73	1.85
Skull	0.018	0.014	0.002	0.1
Scalp	0.44	0.2	0.05	1.0

With the possible exception of the cerebrospinal fluid (CSF), the variability in these data are greater than the precision thought to be required for accurate EEG analysis [1,11,12,15]. Nevertheless, most researchers continue to take conductivity parameters from these standard references, presumably because there is no better method currently available.

We have therefore developed a method of in vivo regional head tissue conductivity estimation, which can easily be applied to individual subjects [4]. In this method, suggested previously by Eriksen [3], a dense-array EEG net is placed on the head surface, and small (1–10 mA) sinusoidal currents are injected into the head volume through selected pairs of electrodes. By measuring the scalp potential at each of the remaining electrodes, regional head tissue conductivities can be determined by inverse methods. The obvious concern with this approach is that, since the low skull conductivity causes most of the injected current to be shunted through the scalp, the sensitivity of the scalp potentials to the inner tissue conductivities (brain and CSF) is necessarily limited. Despite this physical limitation, we present here an inverse procedure that can retrieve all four regional head tissue conductivities to within a few percent error.

2. Methods

2.1 Data acquisition

The proposed method of conductivity estimation is designed to be closely integrated with dense-array EEG data acquisition. Electric current can easily be delivered through any pair of electrodes in the GSN. The Net Amps system is already capable of injecting small currents into the scalp, and such a method is already being used at the beginning of data acquisition to estimate scalp-electrode impedance. By injecting sinusoidal current and averaging over many cycles, the background EEG can be reduced to negligible error. We discuss other noise sources below.

2.2 Forward problem

To address the main problem posed by the low skull conductivity, we focused here on the development of effective inverse methods within a spherical head model. Assuming that the frequency of the injected current is low (f d 1 kHz), the potentials at each time point can be computed as if the current were constant in time. Standard methods show that the scalp potential is given by

$$\Phi(\vec{r}) = \sum_{l=1}^{\infty} A_l [P_l(\cos \theta_A) - P_l(\cos \theta_B)]$$

where θ_A (θ_B) is the angle between the measurement electrode and the positive (negative) injection electrode [4,13]. The constants A_l depend nonlinearly on the four head radii and the four conductivities σ , and linearly on the magnitude of the injected current I . Taking $I = 1 \mu\text{A}$ results in potentials ranging between $\pm 50 \mu\text{V}$ over the scalp surface, depending on the angle between the injection electrodes. On a 300 MHz Macintosh G3, our numerical implementation of the forward solution required approximately 1.8 seconds to compute the potentials for a 128-channel net. This code was written with more emphasis on precision than on speed, however, and we expect that considerable speed increases can be attained with reasonable effort.

2.3 Inverse problem

Due to the algebraic complexity of the coefficients A_l , it is not possible to solve explicitly for the conductivities σ s in terms of the scalp potentials. Instead, inverse methods must be applied. To guide the inverse solution, we defined an error function

$$E_{AB} = \sqrt{\frac{1}{N-2} \sum_{j=1; j \neq A, B}^N (\Phi_j - V_j)^2}$$

where N is the number of scalp electrodes, F_j and V_j are the computed and measured scalp potentials, and A and B refer to the positive and negative injection electrodes, respectively. For a given data set V_j , the best-fit conductivities are those for which E_{AB} is globally minimum. While it is not possible to visualize E_{AB} in the full four-dimensional parameter space, it is still useful to visualize it as a function of each of the four conductivities individually. The different lines in Figure 2 represent electrode separation angles of 32 (dot-dashed), 90 (dashed) and 180 (solid) degrees.

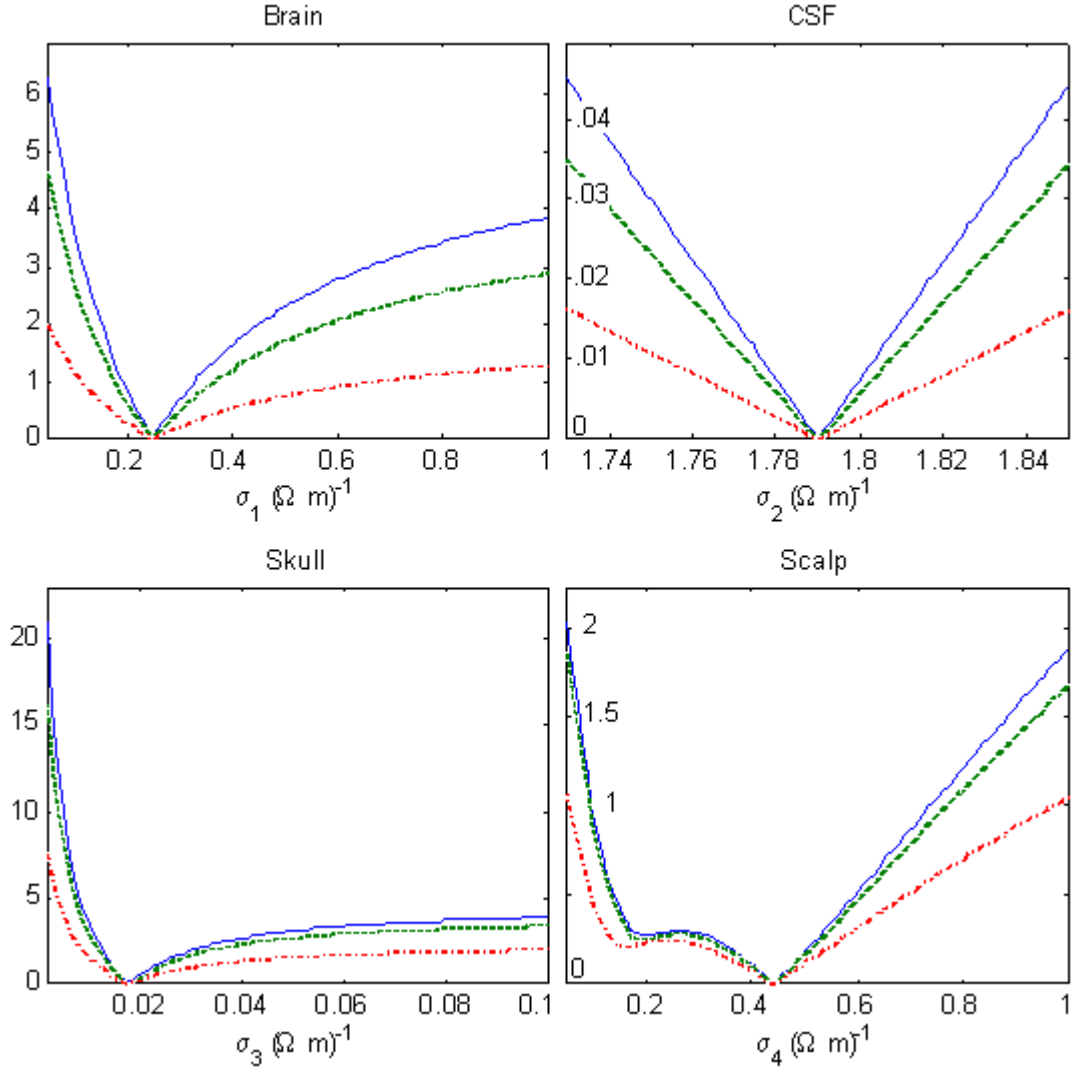


Figure 2. Root-mean-squared error in scalp potentials (μV) as a function of each head tissue conductivity in a four-sphere model of the human head, assuming $1 \mu\text{A}$ injected current.

In each dimension, the error function shows a distinct global minimum. Assuming that this simple structure persists in the four-dimensional space, the goal of the inverse procedure is to find this global minimum, even in the presence of inevitable measurement noise. In preliminary studies, we found that retrieval accuracy was improved by using multiple injection pairs and averaging the corresponding error functions.

$$E = \langle E_{AB} \rangle$$

where the average is computed over a specified set of injection pairs. This improvement is presumably due to the fact that different electrode separation angles generate different current densities in the head volume, and thereby probe the tissues differently. An additional improvement undoubtedly results simply from averaging over different instances of measurement noise, although this effect alone is not sufficient to explain the improvement. In the results described below, we averaged over four injection pairs with electrode separations equal to 48, 94, 130, and 171 degrees.

2.4 Noise

To minimize the error function E as a function of the four conductivities s , we used the downhill simplex algorithm of Nelder and Mead [9]. For each run of the algorithm, the

simplex was initialized randomly by picking four points normally distributed about their mean values, according to the parameters listed in Table 1. To demonstrate conductivity retrieval in computer simulation, we first generated mock scalp data using the mean conductivities listed in Table 1. To make the demonstration more realistic, we added noise to the mock data

$$V_i \rightarrow V_i + n_i$$

where n_i is a zero-mean Gaussian random variable with standard deviation dV , assumed to be uncorrelated across electrodes. By averaging over many cycles of the injected current, the background EEG contributes negligible error. The Net Amps, however, can be expected to contribute noise on the order of $dV=0.1\text{mV}$. Errors due to the misrepresentation of head geometry and electrode placement will be spatially correlated, and are deferred for future study. In studying retrieval accuracy, therefore, we considered noise levels up to $dV = 0.5\text{mV}$. Note that increasing the injected current improves the signal-to-noise ratio in the first two cases only.

3. Results

3.1 Retrieval accuracy

Figure 3 shows the distribution of retrieved conductivities for 50 runs of the simplex algorithm, assuming the noise level $\delta V = 0.1 \mu\text{V}$. Due to the random starting simplex and random noise, each run of the simplex algorithm yields a slightly different result.

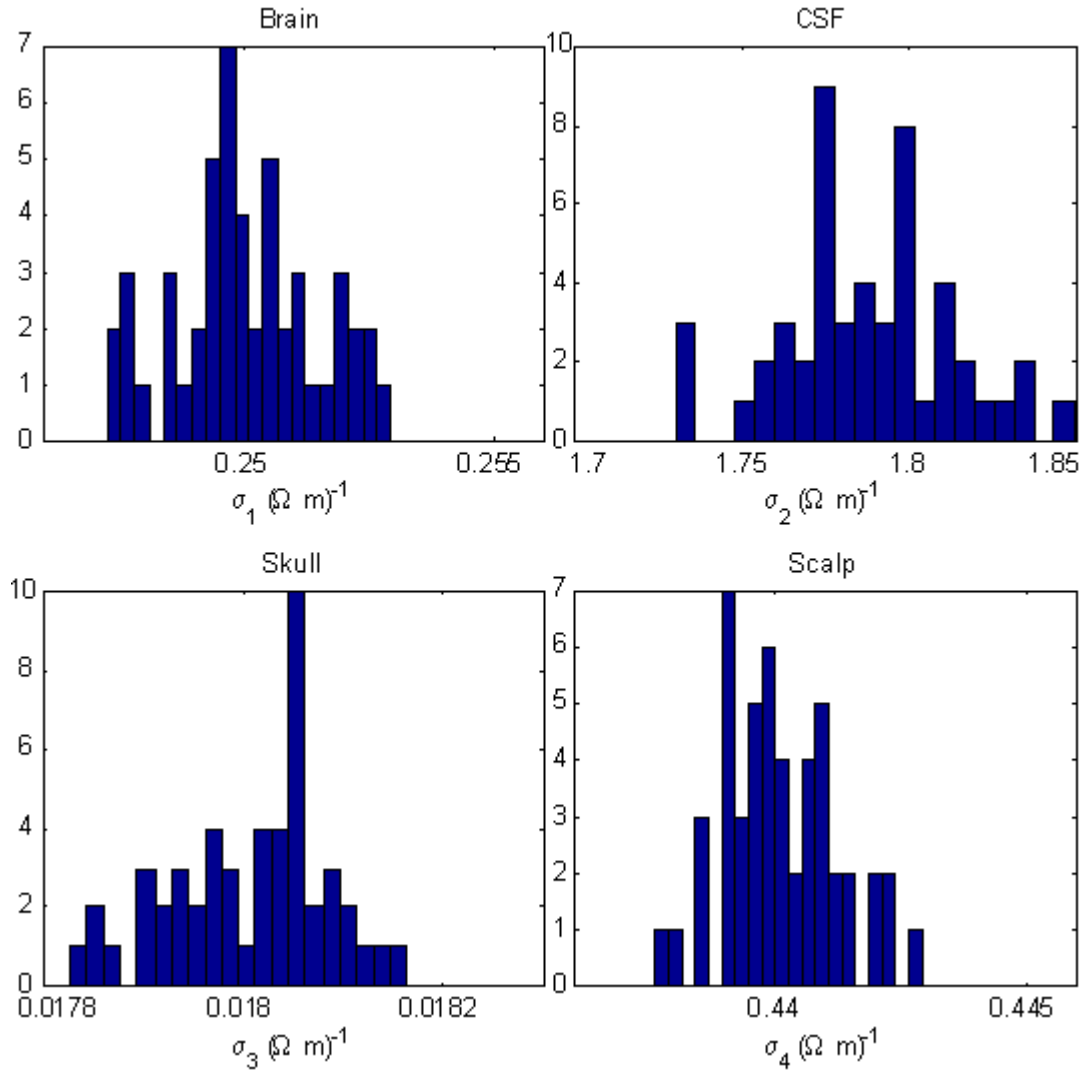


Figure 3. Distribution of retrieved head tissue conductivities in a four-sphere head model, assuming the injected current $I = 1 \mu A$ and the noise level $\delta V = 0.1 \mu V$.

Figure 3 shows that, for each tissue, the distribution of results is sharply peaked about the correct result, and the widths of the distributions are on the order of less than one percent. More precisely, the corresponding retrieval errors for the four tissues are $0.01 \pm 0.6\%$ (brain), $-0.13 \pm 1.4\%$ (CSF), $0.03 \pm 0.43\%$ (skull), and $0.02 \pm 0.26\%$ (scalp). This suggests that, despite the low skull conductivity, it is entirely feasible to measure the average regional conductivity of the brain, CSF, skull and scalp using scalp current injection.

3.2 Multi-start interpretation

The distributions in Figure 3 can be interpreted in two ways. If the simplex algorithm were run only once, then these distributions would show the range of retrieval errors. On the other hand, if the results of the 50 runs are taken together, then the means of the distributions yield much more accurate estimates. Using the result of many runs in this way can be viewed as a multi-start method, not unlike that used in dipole source localization [6]. For example, if the means in Figure 3 are taken to provide the true estimate, then this method produces estimates of regional conductivities with errors on the order of 0.1% for the CSF, and on the order of 0.01% for the remaining tissues.

3.3 Dependence on noise level

As the noise level increases, the retrieval accuracy degrades, as expected. Even when the

noise level is $dV=0.5\text{mV}$, however, this multi-start method produces a distribution of results for which the error of the mean is still on the order of only 0.5% for each tissue. Such graceful degradation with noise is a highly sought-after feature of computer algorithms intended for real-world use.

4. Discussion

We have developed a method of in vivo head tissue conductivity estimation using scalp current injection. Together with anatomical data from structural MRI, these results can be used to build more accurate head models, which could substantially improve dense-array EEG data analysis. The fact that the method uses the same EEG acquisition system makes it both convenient and cost effective. In practice, current injections could be made when the GSN is placed on the subject's head, and the inverse solution for regional head tissue conductivities could be computed later during off-line data analysis.

In retrospect, it is easy to understand why this method works. First, since the current source is known, this inverse problem does not suffer from the issues of non-uniqueness which plague dipole source localization. Hence the error function appears to have a distinct global minimum in the absence of noise. Second, the addition of random noise to the data introduces local minima into the error function, making perfect retrieval difficult or impossible. Practically speaking, however, retrieval accuracy depends upon how severely these local minima distort the shape, and especially the location of the center, of the global basin of attraction. For the parameter ranges and noise levels relevant to this problem, the general shape of the error function is apparently preserved. This allows a clustering of solutions in the vicinity of the correct answer and, by computing their mean, a very accurate estimate is obtained. As a bonus, the distribution of results generated in this multi-start approach provides confidence intervals, which would not be available from a single search attempt.

Current research efforts are aimed at using global search algorithms to find the optimal solution in less iterations, developing boundary element and finite element methods to incorporate realistic head geometry, and generalizing this approach to detect local changes in tissue impedance which might signify pathological states of brain tissue.

Acknowledgements

The authors gratefully acknowledge that this work was supported by NIMH 2-R43-MH-53768-02.

References

- [1] Awada, K. A., D. R. Jackson, S. B. Baumann, J. T. Williams, D. R. Winton, P. W. Fink, and B. R. Prasky (1998). Effect of conductivity uncertainties and modeling errors on EEG source localization using a 2-D model. *IEEE Transactions on Biomedical Engineering* 45(9):1135-1145.
- [2] Baumann, S. B., D. R. Wonzy, S. K. Kelly and F. M. Meno (1997). The electrical conductivity of human cerebrospinal fluid at body temperature. *IEEE Transactions on Biomedical Engineering* 44(3): 220-223.
- [3] Eriksen, K. J. (1990). In vivo head regional conductivity estimation using a three-sphere model. *Proceedings of the Annual International Conference of the IEEE Engineering in Medicine and Biology Society* 12(4): 1494-1495.
- [4] Ferree, T. C., K. J. Eriksen and D. M. Tucker (1999). In vivo head tissue conductivity estimation using scalp current injection. Submitted to *IEEE Transactions on Biomedical Engineering*.
- [5] Geddes, L. A. and L. E. Baker (1967). The specific resistance of biological materials: A compendium of data for the

biomedical engineer and physiologist. *Med. Biol. Eng.* 5: 271-293.

- [6] Huang, M., C. J. Aine, S. Supek, E. Best, D. Ranken, and E. R. Flynn (1998). Multi-start downhill simplex method for spatio-temporal source localization in magnetoencephalography. *Electroencephalography and Clinical Neurophysiology* 108: 32-44.
- [7] Law, S. K. (1993). Thickness and resistivity variations over the upper surface of the human skull. *Brain Topography* 6(2): 99-109.
- [8] Luu, P., D. M. Tucker, T. C. Ferree, R. Englander, A. Lockfeld, and H. Lutsep (1999). Clinical interpretation of stroke-related EEG is enhanced by dense-array spatial sampling: characterization of stroke-related EEG topography. In preparation.
- [9] Press, W. H., S. A. Teukolsky, W. T. Vetterling and B. P. Flannery (1992). *Numerical recipes in C*. Cambridge University Press.
- [10] Oostendorp, T. and A. van Oosterom (1991). The potential distribution generated by surface electrodes in inhomogeneous volume conductors of arbitrary shape. *IEEE Transactions on Biomedical Engineering* 38(5): 409-417.
- [11] Laarne, P., P. Kauppinen, J. Hyttinen, J. Malmivuo, and H. Eskola. Effects of tissue resistivities on EEG sensitivity distribution. Submitted to *Medical and Biological Engineering and Computing*.
- [12] Pilkington, T. C., and R. Plonsey (1982). *Engineering Contributions to Biophysical Electrocardiography*. IEEE, New York.
- [13] Rush, S. and D. A. Driscoll (1969). EEG electrode sensitivity - an application of reciprocity. *IEEE Transactions on Biomedical Engineering* 16(1): 15-22.
- [14] Srinivasan, R., D. M. Tucker and M. Murias (1998). Estimating the spatial nyquist of the human EEG. *Behavior Research Methods, Instruments, and Computers* 30: 8-19.
- [15] Stok, C. J. (1987). The influence of model parameters on EEG/MEG single dipole source estimation. *IEEE Transactions on Biomedical Engineering* 34(4): 289-296.
- [16] Tucker, D. M. (1991). Spatial sampling of head electric fields: The geodesic sensor net. *Electroencephalography and Clinical Neurophysiology* 79: 413



Official journal of the [International Society for Bioelectromagnetism](#)